ACS Macro Letters

Letter

pubs.acs.org/macroletters

Self-Organized Columnar Phase of Side-Chain Liquid Crystalline Polymers: To Precisely Control the Number of Chains Bundled in a Supramolecular Column

Xiao-Qing Liu, Jun Wang, Shuang Yang,* and Er-Qiang Chen*

Beijing National Laboratory for Molecular Sciences, Key Laboratory of Polymer Chemistry and Physics of Ministry of Education, College of Chemistry, Peking University, Beijing 100871, China

Supporting Information

ABSTRACT: Self-organization of liquid crystalline (LC) polyacetylene derivatives (PAs) bearing hemiphasmid side-chains was investigated. The synthesized PAs can form smectic and columnar phases, depending on the constitutions of side chains. With a nanosegregation structure, the columnar phase of PAs takes a bundle of chains as its building block, of which the chain number is precisely determined by the volume fraction of the rigid component in PAs. The "precise multi-chain column" can be understood using a mean field theory, from which the deduced number of chains in the supramolecular column agrees well with the experimental result. This study reveals that the volume fraction of the rigid component plays a significant role in the self-organization of side-chain LC polymers, which is valuable for the rational design of macromolecules with precisely ordered structures.

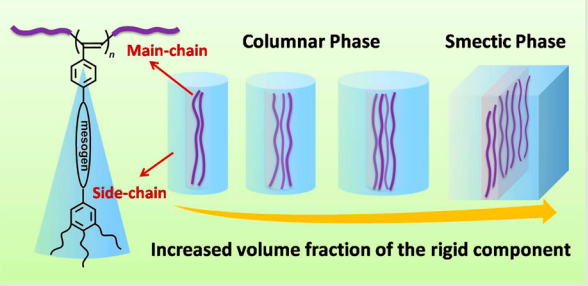

Side-chain liquid crystalline polymers (SCLCPs) with well-defined supramolecular shapes constitute a powerful platform for creating nanastructures 5−10 nm in size, showing great potential in nanomaterials and nanotechnology.[1−3] Typical shape-persistent SCLCPs, such as mesogen-jacketed liquid crystalline (LC) polymers[4] and dendronized polymers,[5] tend to self-organize into columnar (Φ) structures in which the whole macromolecules serve as the anisotropic building blocks.[6] The cylindrical building block in the Φ phase has attracted considerable interest for the design of highly ordered structures[7,8] and also for the applications such as ionic transportation.[9,10]

Self-organization of cylindrical macromolecules is generally driven by nanosegregation occurring among the incompatible chemical components in the supramolecular column of SCLCPs.[11,12] An intracolumnar microphase-segregated model has been used to describe the core−shell structure of a cylindrical macromolecule. For example, in dendronized polymers developed by Percec et al., tapered side groups of a macromolecule assemble into cylindrical shape with the backbone penetrating through the cylinder center.[5,13] However, it actually remains unclear whether the supramolecular column is composed of a single-chain or a bundle of chains, which is a critical character of the Φ structure.[6,14]

While a single-chain column is mostly accepted as the building block of the Φ phase, multi-chain column has also been suggested in some cases. In the supramolecular system of rodlike bolaamphiphiles with lateral swallow-tailed chains, axial-bundle Φ phases are formed by bundles of several parallel rods.[14−16] Hairy-rod polymers,[17] such as cellulose trialkanoates[18] and poly(*n*-alkyl glutamate)s with long side chains,[19] form supramolecular columns with two-intertwined chains in Φ phase. ten Brinke et al. have theoretically predicted a hexagonal structure characterized by cylindrical micelles containing several hairy-rod polymers.[20] Recently, we studied a series of polystyrene derivatives bearing hemiphasmid side chains,[21] which consist of a rodlike mesogen and a "half-disc" end group.[11,22−25] We consider that a bundle of chains constitutes the supramolecular column of hemiphasmid SCLCPs.[21] This "multi-chain column" is in agreement with the packing scheme suggested by Ungar.[6] Yet, the challenge in the "multi-chain column" is to precisely control the number of chains associated in the supramolecular column.

In the present work of hemiphasmid SCLCPs with polyacetylene (PA) backbone, we demonstrate that the number of bundled chains in the "multi-chain column" can be facilely tuned by the volume fraction of the rigid component in the polymer. The semirigid PA backbone endows the polymer with greater shape persistency.[26−31] PA derivatives bearing functional side-chains can exhibit fantastic LC, electronic, optical, and biological properties.[32] Chemical structures of five PA derivatives (PAs) studied here are shown in Chart 1. Among them, PA2, PA1, and PA0 with reduced sizes of the aromatic group on side-chains have been reported.[33] The alkyl group varies from C8 in PA2 to C4 and C12 in PA2a and PA2b, respectively. For PA2, PA1, and PA0 in Φ phases, the

Received: June 30, 2014
Accepted: August 7, 2014
Published: August 11, 2014

   dx.doi.org/10.1021/mz500387a | *ACS Macro Lett.* 2014, 3, 834−838

Chart 1. Chemical Structures of PAs

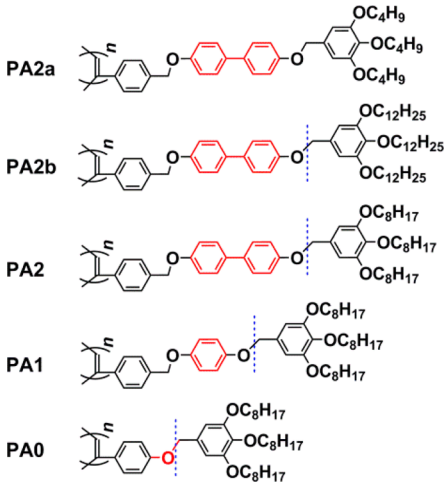

supramolecular columns are found to include exactly 4, 3, and 2 chains, respectively. With such a "precise multi-chain column", we intend to address how the constitution of side-chain affects the chain packing behavior in Φ phases of SCLCPs. A theoretical approach to this issue will also be demonstrated.

PAs with a high *cis* stereoregularity of the main chain were synthesized using Rh catalyst.[33] Detailed synthesis and characterization of PAs are given in the Supporting Information (Tables S1 and S2 and Figure S1). LC phases of thermally annealed PAs were identified using X-ray diffraction (XRD) method. As shown in Figure 1a, PA2a with short alkyl tails

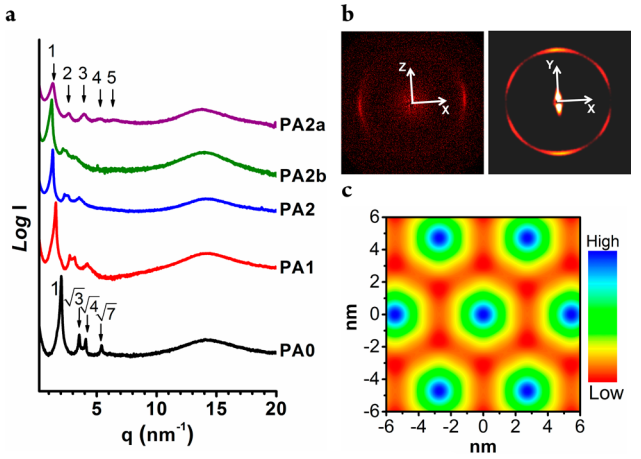

Figure 1. Phase structure characterization of PAs. (a) XRD profiles of PAs recorded at room temperature. (b) 2D XRD patterns of sheared PA2. Left and right panel: X-ray incident beam are parallel to the shear gradient (*Y*-direction) and the shear direction (*Z*-direction), respectively. Only the first (10) diffraction of PA2 can be detected while the others are beyond the detection limit of the equipment. (c) Reconstructed electron density map of PA2. The phases of four hexagonal diffractions were assigned to be ++++. The length unit is nm.

forms a smectic (Sm) phase, which is characterized by the low-angle reflections with a *q*-ratio of 1:2:3:4:5 ($q = 4\pi \sin\theta/\lambda$, with λ the X-ray wavelength and 2θ the scattering angle). For other four PAs, the *q*-ratio of $1:\sqrt{3}:\sqrt{4}:\sqrt{7}$ clearly suggests a hexagonal Φ (Φ_H) phase. The glass transition temperatures (T_g) of PAs are relatively low (Table S2). The samples were easily oriented by mechanical shearing at above T_g, which enabled us to elucidate the Φ_H phase by two-dimensional (2D) XRD experiment of the sheared samples. Taking PA2, for example, when the X-ray incident beam is perpendicular to the shear direction (*Z*-direction), the (10) diffraction of PA2 locates on the horizontal line, suggesting that the polymer chains are well oriented along the shear direction. Moreover, 6-fold symmetry of (10) diffraction can be observed when the X-ray beam goes through the shear direction. Therefore, the columns lie well down in the shear plane. 2D XRD patterns of PA1 and PA0 also indicated clearly the Φ_H phase (Figure S2). Our XRD results reveal that the LC structures of PAs can be tuned by the constitutions of side chains. Increasing the length of alkyl tails leads to a transition from Sm to Φ_H (LC textures shown in Figure S3). Decreasing the size of aromatic group in side chains reduces the unit cell parameter of Φ_H phase from 5.49 nm of PA2 to 3.56 nm of PA0 (Table 1).

Table 1. LC Phase Identification, Phase Structure Dimension, and Calculation of the Number of Chains in a Column of PAs Based on the Experimental Results

	LC phase	M_{rep}[a] (g/mol)	d[b] (nm)	ρ[c] (g/cm³)	m[d]	Q[e]
PA2a	Sm	606.8	4.69	1.120		
PA2b	Φ_H	943.4	6.15	1.016	4.25	4
PA2	Φ_H	775.1	5.49	1.023	4.15	4
PA1	Φ_H	699.0	4.59	0.994	3.12	3
PA0	Φ_H	592.9	3.56	0.955	2.13	2

[a]Molar mass of repeating units. [b]Experimentally determined layer spacing of Sm phase and unit cell parameter of the Φ_H phase. [c]Experimental densities of PAs. [d]Numbers of repeat units in a column stratum with a thickness (t) of 2 Å. [e]Deduced number of chains in each column.

Similar to that of dendronized polymers, self-organization of PAs is dominated by nanosegregation between flexible alkyl tails and the rigid domain involving the backbone and rodlike mesogens. Reconstructed electron density maps[21] of PAs show a clear core−corona structure of the column in the Φ_H phase (Figure 1c and Figure S4). Considering that increasing the alkyl tail length changes the LC structure from Sm to Φ_H, the most probable packing scheme for the Φ_H should be that the rigid part locates in the core (blue and green colored region), while alkyl tails occupy the corona (red colored region) as the continuous phase. We failed to directly observe this structure by transmission electron microscopy on selectively stained or oriented samples because the samples were extremely unstable under the electron beam. Nevertheless, an inverted morphology[34−36] with alkyl tails in the cylinder core is not applicable here, because it is energetically unfavorable for the semirigid main chains (Figure 2) to form a continuous phase confining the alkyl tails inside the cylinder.

To verify the possible "multi-chain column" model in the Φ_H phase of the hemiphasmid PAs, the number of repeating units m in a unit stratum of the column was first estimated in terms of $m = (N_A/M_{rep})(d^2t \sin 60°)\rho$ with N_A the Avogadro's number, ρ the density, t the column stratum thickness, and M_{rep} the molar mass of the repeating unit.[21] As the Φ phase is disordered along the column axis,[6] the value of t can be assigned arbitrarily. Taking t of 2 Å, the calculated values of m are 4.15 and 4.25 for PA2 and PA2b, respectively (Table 1), which means that approximately four repeating units are arranged in a stratum as thin as 2 Å. Considering the local

dx.doi.org/10.1021/mz500387a | ACS Macro Lett. 2014, 3, 834−838

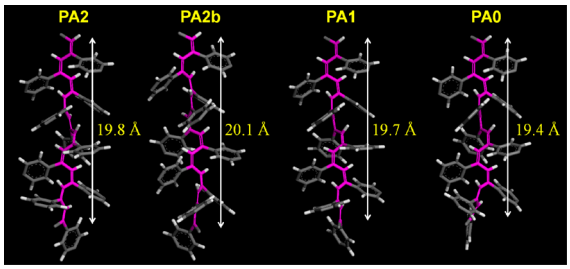

Figure 2. Models illustrating chain lengths of PAs with 10 repeating units after geometry optimization. The chain lengths are 19.8, 20.1, 19.7, and 19.4 Å for PA2, PA2b, PA1, and PA0, respectively. Only the poly(phenylacetylene) main-chain was shown for clarity.

rigidity of the PA backbone, it is incomprehensible to squeeze four repeating units of a single chain into such a small thickness. Most likely, the repeating units come from a bundle of chains in the column.

Actually, we chose the value of 2 Å for t based on the following reasons. Previous study on the crystal structure of *cis*-PA has revealed an orthorhombic unit cell with c = 4.38 Å (two repeating unit), in which the polymer chain has a 2_1 screw axis.[37] Assuming that the PA backbone adopts an extended *cis*-transoidal conformation (Figure 2), molecular simulation about the single chain of PAs with 10 repeating units shows that the optimized chain length is about 20 Å, irrespective of the side-chain structures (Figures S5 and S6). Thus, t of 2 Å can be regarded as the projection length of each repeating unit on the PA backbone. In this context, the number of repeating units packing in a 2 Å-thick stratum is equivalent to the number of chains (Q) involved in the supramolecular column. Using t = 2 Å, the calculated m is listed in Table 1. For PA1 and PA0, the m values are of 3.12 and 2.13, respectively. Considering the integer number Q of the multichain, it is naturally concluded that the column of PA2, PA1, and PA0 contains 4, 3, and 2 chains, respectively. For PA2b, Q should be 4, the same as that of PA2. Note that Q decreases on reducing the size of the aromatic part in the side chain. It indicates that the volume fraction of the rigid part plays a critical role in the formation of multichain column in PAs, analogous to the cases in block copolymers[38] and hairy-rod polymers.[20] To elucidate why the system adopts specific number of chains to form a "precise multi-chain column", we employ a mean field theory to analyze the equilibrium state of the Φ_H structure of PAs.

Like the treatment applied in hairy-rod polymer,[20] the molecules of PAs can be divided into two regions as indicated by the blue dashed lines in Chart 1. One is the rigid part involving the main-chain and mesogenic part of side group (rod) and the other is the flexible alkyl tails (hairy). The chain is coarsely grained into a rod with a length of H bearing M side chains equidistantly grafted with a density of $1/b$ ($b = H/M$). The radius of the cylindrical polymer is R_0, of which the rigid core has a radius r_0 ($r_0 \ll H$; Figure 3a). For the outer corona, as a rough approximation, the flexible part is assumed to be a coil bearing N beads, and the bead occupies a volume v and has a statistical segment length a. The volume fraction of rigid core is $f_0 = (r_0/R_0)^2$, and that of corona is $1 - f_0$.

Taking a blend of pure nematic phase of rigid rods and pure melt of flexible coils as a reference state, the orientational entropy of rigid rods is nearly unvaried and can be ignored since they are always aligned.[20] Then the free energy of each coarse grained chain is expressed as

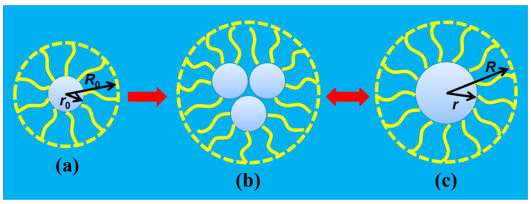

Figure 3. Schematic representation of the supramolecular cylinder in the Φ_H phase. (a) Single-chain column with a dimension R_0 consists of the inside rigid domain (core, r_0) and the outer aliphatic domain. (b) A bundle of chains associates together in the "multi-chain column". (c) Multichain in (b) can be regarded as a new cylinder with a dimension R. The inside rigid domain (core) possesses a radius of r.

$$F = F_{el} + F_{int} \tag{1}$$

where F_{el} is the elastic stretching energy of tails, dominated by the conformational entropy of flexible side chains, and F_{int} is the interfacial free energy of the core−corona interface. The second term is the product of interfacial tension γ and interfacial area:

$$F_{int} = 2\pi r_0 H\gamma \tag{2}$$

Assuming that the flexible side chains are long enough and strongly separated from the main chains, they tend to be strongly stretched to reach minimum contacting with the rodlike main chains, similar to the situation of block copolymer systems. In this case, as an approximation, F_{el} can be obtained by use of the strong stretching theory[39,40] and reads

$$\frac{F_{el}}{k_BT} = \frac{3\pi}{8}\frac{R_0^4 H(1-f_0)^2}{a^2 v N^2}\ln\left(\frac{1}{f_0}\right) \tag{3}$$

The equilibrium phase of the system is determined by the competition between F_{el} and F_{int}. When F_{el} is much larger than F_{int}, the Φ_H phase with single-chain column can be found. Oppositely, if γ is large enough and f_0 is not too small, the Sm phase appears to minimize the interfacial area (such as PA2a with f_0 of 42.2%). In the intermediate regime, another Φ_H phase with multichain column may be realized, which is predicted for the self-organization of hairy-rod polymers by ten Brinke et al.[20]

For the chains bundled together in a column, we further presume that side-chains from different backbones can intersperse with each other, leading to a "fused" rigid domain. Figure S7 gives a snapshot of two "fused" chains of PA0, showing a possible arrangement of backbones and the side-chains. In this case, the new column has an effective core radius of r and a total radius of R (Figure 3), with the following relationships satisfied:

$$r^2 = Qr_0^2;\quad R^2 = QR_0^2 \tag{4}$$

The volume fraction of the core in the new column, f, is unchanged, that is, $f = f_0$. The volume of the corona now reads:

$$\pi[R^2(1-f)]H = QMNv \tag{5}$$

For the column with several chains "fused" together, eq 3 is still applicable. The free energy of each column is given by

$$\frac{F}{k_BT} = \frac{2\pi Hr\gamma}{k_BT} + \frac{3\pi}{8}\frac{R^4 H(1-f)^2}{a^2 v N^2}\ln\left(\frac{1}{f}\right) \tag{6}$$

Using eqs 4−6, the free energy per molecule per unit length (g) can be expressed as

dx.doi.org/10.1021/mz500387a | ACS Macro Lett. 2014, 3, 834−838

$$g = \frac{2\pi r_0 \gamma}{k_B T \sqrt{Q}} + \frac{3\pi}{8}\frac{Q v}{a^2 b^2} \ln\left(\frac{1}{f_0}\right) \quad (7)$$

Thus, the associated chain number Q at equilibrium can be estimated from the free energy minimization at $\partial g/\partial Q = 0$, that is,

$$Q = \left(\frac{3\pi}{8}\frac{a^2 b^2 r_0 \gamma / k_B T}{v \ln(1/f_0)}\right)^{2/3} \quad (8a)$$

This expression demonstrates the dependence of Q on the size r_0 and the volume fraction f_0. It captures the main feature of the column with a core−corona structure and has wide applicability even for short side chains. We use eq 8 to analyze the chain numbers in PA2, PA1, and PA0, of which the sizes of rigid cores vary while the flexible tails remain the same. As γ can be regarded as constant, eq 8a is simplified to

$$Q \propto \left(\frac{r_0}{\ln(1/f_0)}\right)^{2/3} \propto \left(\frac{\sqrt{M_1/\rho_1}}{\ln(1 + M_2\rho_1/M_1\rho_2)}\right)^{2/3} \quad (8b)$$

Here M_1 (ρ_1) and M_2 (ρ_2) denote the molar mass (density) of the rigid part in the core and that of the flexible part in the corona per repeat unit, respectively.

With a reasonable assumption of $\rho_2 \approx 0.90$ g·cm^{-3} and measured density of PAs (Table 1), ρ_1 is estimated to be of ∼1.20 g·cm^{-3}, which is in the acceptable range.[11] Then, the calculated volume fractions of the core are 32, 26, and 16% for PA2, PA1, and PA0, respectively (Table 2). Consequently, the

Table 2. Calculation of the Chain Numbers in Each Column of Φ_H Phases of PAs

	M_1[a] (g/mol)	M_2[b] (g/mol)	f_0[c] (%)	"Q"[d]	Q-ratio
PA2	299.3	475.7	32.1	5.78	1.90
PA1	223.2	475.7	26.0	4.68	1.54
PA0	117.1	475.7	15.6	3.04	1.00

[a]Molar mass of the rigid core. [b]Molar mass of the flexible corona. [c]Calculated volume fraction of the core in the column based on the estimated density (ρ_1 and ρ_2 are 1.20 and 0.90 g·cm^{-3}, respectively). [d]The number of chains (Q) in a column is proportional to the corresponding value of "Q", which is calculated according to eq 8b.

Q-ratio of PA2, PA1, and PA0 can be calculated as 1.90:1.54:1.00 (Table 2), which agrees well with that obtained from experiments (4:3:2). This astonishing coincidence between theory and experiment makes us believe that the "precise multi-chain column" embodies the real microstructure of the columnar phase. Equation 8 predicts that the Q-ratio between PA2b and PA2 is of 0.89:1.00, suggesting that 3.5 chains are included in one PA2b cylinder in the equilibrated state. Thus, four chains in PA2b's column according to the experimental data may correspond to a metastable state. Compared to PA1, PA2b possesses an almost same f_0 of 25.8%, however, its relatively larger r_0 leads to a larger Q.

According to eq 8, the chain number Q in a column will eventually reach one when r_0 (or f_0) is further decreased, and thus, the chain packing scheme reduces to the "single-chain column". Although this cannot be observed in our PAs samples, using the data reported,[41] the "single-chain column" can be identified in the dendronized PAs with the half disk moieties similar to ours, where the volume fraction of rigid component is about 4−5% (Part 8 in SI).

In conclusion, we have shown that hemiphasmid SCLCPs with polyacetylene backbone can self-organize into Sm and Φ_H phases. In the Φ_H phase, the supramolecular column consisting of a bundle of chains is the LC building block. This is a consequence of the balance between the interfacial interaction of two incompatible components (rigid and flexible parts) and the elastic stretching energy of alkyl tails. Importantly, the number of bundled chains reduces with decreased volume fraction of the rigid component, which has been realized in our work by decreasing the size of the aromatic part on side chains. When the volume fraction of the rigid component is reduced to about 5% (e.g., in dendronized polymers), the Φ_H phase with single-chain as its building block can appear. The revealed microstructure formation mechanism in this study will be of value for better understanding columnar phase in side-chain polymers featured with a bundle of chains associated laterally together and, thus, be helpful for precise fabrication of macromolecules with highly ordered structure approaching the dimension of 10 nm.

■ ASSOCIATED CONTENT

Supporting Information

Experimental details, synthesis and characterizations of PA2a and PA2b, DSC curves, 2D XRD patterns, and LC textures of PAs, relative electron density reconstruction, molecular simulation of PAs, and comparison of hemiphasmid PA with dendronized PAs. This material is available free of charge via the Internet at http://pubs.acs.org.

■ AUTHOR INFORMATION

Corresponding Authors

*E-mail: eqchen@pku.edu.cn.

*E-mail: shuangyang@pku.edu.cn.

Notes

The authors declare no competing financial interest.

■ ACKNOWLEDGMENTS

We thank Prof. An-Chang Shi for the helpful discussion, Dr. Song Hong for the TEM observation. This work was supported by the National Natural Science Foundation of China (NNSFC Grants 51273002, 20990232, and 21104001).

■ REFERENCES

(1) Percec, V.; Ahn, C. H.; Ungar, G.; Yeardley, D. J. P.; Möller, M.; Sheiko, S. S. *Nature* **1998**, *391*, 161−164.

(2) Sheiko, S. S.; Sumerlin, B. S.; Matyjaszewski, K. *Prog. Polym. Sci.* **2008**, *33*, 759−785.

(3) Zhang, B.; Wepf, R.; Fischer, K.; Schmidt, M.; Besse, S.; Lindner, P.; King, B. T.; Sigel, R.; Schurtenberger, P.; Talmon, Y.; Ding, Y.; Kröger, M.; Halperin, A.; Schlüter, A. D. *Angew. Chem., Int. Ed.* **2011**, *50*, 737−740.

(4) Chen, X. F.; Shen, Z. H.; Wan, X. H.; Fan, X. H.; Chen, E. Q.; Ma, Y. G.; Zhou, Q. F. *Chem. Soc. Rev.* **2010**, *39*, 3072−3101.

(5) Rosen, B. M.; Wilson, C. J.; Wilson, D. A.; Peterca, M.; Imam, M. R.; Percec, V. *Chem. Rev.* **2009**, *109*, 6275−6540.

(6) Ungar, G. *Polymer* **1993**, *34*, 2050−2059.

(7) Hosono, N.; Kajitani, T.; Fukushima, T.; Ito, K.; Sasaki, S.; Takata, M.; Aida, T. *Science* **2010**, *330*, 808−811.

(8) Bong, D. T.; Clark, T. D.; Granja, J. R.; Ghadiri, M. R. *Angew. Chem., Int. Ed.* **2001**, *40*, 988−1011.

(9) Yoshio, M.; Kagata, T.; Hoshino, K.; Mukai, T.; Ohno, H.; Kato, T. *J. Am. Chem. Soc.* **2006**, *128*, 5570−5577.

(10) Marcos, M.; Martin-Rapun, R.; Omenat, A.; Serrano, J. L. *Chem. Soc. Rev.* **2007**, *36*, 1889−1901.
(11) Ungar, G.; Abramic, D.; Percec, V.; Heck, J. A. *Liq. Cryst.* **1996**, *21*, 73−86.
(12) Soininen, A. J.; Kasëmi, E.; Schlüter, A. D.; Ikkala, O.; Ruokolainen, J.; Mezzenga, R. *J. Am. Chem. Soc.* **2010**, *132*, 10882−10890.
(13) Rudick, J. G.; Percec, V. *Acc. Chem. Res.* **2008**, *41*, 1641−1652.
(14) Liu, F.; Prehm, M.; Zeng, X.; Ungar, G.; Tschierske, C. *Angew. Chem., Int. Ed.* **2011**, *50*, 10599−10602.
(15) Prehm, M.; Liu, F.; Zeng, X.; Ungar, G.; Tschierske, C. *J. Am. Chem. Soc.* **2011**, *133*, 4906−4916.
(16) Liu, F.; Prehm, M.; Zeng, X.; Tschierske, C.; Ungar, G. *J. Am. Chem. Soc.* **2014**, *136*, 6846−6849.
(17) Wegner, G. *Macromol. Chem. Phys.* **2003**, *204*, 347−357.
(18) Yamagishi, T.; Fukuda, T.; Miyamoto, T.; Takashina, Y.; Yakoh, Y.; Watanabe, J. *Liq. Cryst.* **1991**, *10*, 467−473.
(19) Watanabe, J.; Ono, H.; Uematsu, I.; Abe, A. *Macromolecules* **1985**, *18*, 2141−2148.
(20) Stepanyan, R.; Subbotin, A.; Knaapila, M.; Ikkala, O.; Ten Brinke, G. *Macromolecules* **2003**, *36*, 3758−3763.
(21) Zheng, J. F.; Liu, X.; Chen, X. F.; Ren, X. K.; Yang, S.; Chen, E. Q. *ACS Macro Lett.* **2012**, *1*, 641−645.
(22) Lin, C.; Ringsdorf, H.; Ebert, M.; Kleppinger, R.; Wendorff, J. H. *Liq. Cryst.* **1989**, *5*, 1841−1847.
(23) Percec, V.; Heck, J.; Ungar, G. *Macromolecules* **1991**, *24*, 4957−4962.
(24) Kwon, Y. K.; Chvalun, S.; Schneider, A.; Blackwell, J.; Percec, V.; Heck, J. A. *Macromolecules* **1994**, *27*, 6129−6132.
(25) Kwon, Y. K.; Chvalun, S. N.; Blackwell, J.; Percec, V.; Heck, J. A. *Macromolecules* **1995**, *28*, 1552−1558.
(26) Ye, C.; Xu, G. Q.; Yu, Z. Q.; Lam, J. W. Y.; Jang, J. H.; Peng, H. L.; Tu, Y. F.; Liu, Z. F.; Jeong, K. U.; Cheng, S. Z. D.; Chen, E. Q.; Tang, B. Z. *J. Am. Chem. Soc.* **2005**, *127*, 7668−7669.
(27) Percec, V.; Rudick, J. G.; Peterca, M.; Wagner, M.; Obata, M.; Mitchell, C. M.; Cho, W.; Balagurusamy, V. S. K.; Heiney, P. A. *J. Am. Chem. Soc.* **2005**, *127*, 15257−15264.
(28) Percec, V.; Rudick, J. G.; Peterca, M.; Staley, S. R.; Wagner, M.; Obata, M.; Mitchell, C. M.; Cho, W.; Balagurusamy, V. S. K.; Lowe, J. N.; Glodde, M.; Weichold, O.; Chung, K. J.; Ghionni, N.; Magonov, S. N.; Heiney, P. A. *Chem.—Eur. J.* **2006**, *12*, 5731−5746.
(29) Percec, V.; Peterca, M.; Rudick, J. G.; Aqad, E.; Imam, M. R.; Heiney, P. A. *Chem.—Eur. J.* **2007**, *13*, 9572−9581.
(30) Liu, K. P.; Yu, Z. Q.; Liu, J. H.; Chen, E. Q. *Macromol. Chem. Phys.* **2009**, *210*, 707−716.
(31) Yu, Z. Q.; Lam, J. W. Y.; Zhu, C. Z.; Chen, E. Q.; Tang, B. Z. *Macromolecules* **2013**, *46*, 588−596.
(32) Liu, J. Z.; Lam, J. W. Y.; Tang, B. Z. *Chem. Rev.* **2009**, *109*, 5799−5867.
(33) Liu, X. Q.; Li, Y. L.; Lin, Y. W.; Yang, S.; Guo, X. F.; Li, Y.; Yang, J.; Chen, E. Q. *Macromolecules* **2013**, *46*, 8479−8487.
(34) Canilho, N.; Kasëmi, E.; Schlüter, A. D.; Ruokolainen, J.; Mezzenga, R. *Macromolecules* **2007**, *40*, 7609−7616.
(35) Lee, W. B.; Elliott, R.; Mezzenga, R.; Fredrickson, G. H. *Macromolecules* **2009**, *42*, 849−859.
(36) Mezzenga, R.; Ruokolainen, J.; Canilho, N.; Kasemi, E.; Schluter, D. A.; Lee, W. B.; Fredrickson, G. H. *Soft Matter* **2009**, *5*, 92−97.
(37) Chien, J. C. W.; Karasz, F. E.; Shimamura, K. *Macromolecules* **1982**, *15*, 1012−1017.
(38) Bates, F. S.; Fredrickson, G. H. *Annu. Rev. Phys. Chem.* **1990**, *41*, 525−557.
(39) Semenov, A. N. *Sov. Phys. JETP* **1985**, *61*, 733−742.
(40) Fredrickson, G. H. *Macromolecules* **1993**, *26*, 4351−4355.
(41) Percec, V.; Aqad, E.; Peterca, M.; Rudick, J. G.; Lemon, L.; Ronda, J. C.; De, B. B.; Heiney, P. A.; Meijer, E. W. *J. Am. Chem. Soc.* **2006**, *128*, 16365−16372.